

ENGR241 Fall 2016 Final Report

Optimizing the Electrical Stability of Platinum Films Deposited in Lesker-Sputter

Kirsten Kaplan, Karen Kim, Martin Winterkorn

Mentors: J Provine, Shiva Bhaskaran

Staff Mentors: Maurice Stevens, Carsen Kline

1. Motivation and Goals

Platinum thin films are used in a wide range of applications, despite the raw material's high cost, due to platinum's unique chemical, thermal and electrical properties, such as high corrosion resistance, catalytic activity, high melting temperature, large temperature coefficient of resistivity (TCR) and low intrinsic noise. The latter two factors make platinum particularly attractive for thermistors, which have very widespread usage and are a key component of thermal accelerometers, the particular device application that this study is aimed at.

1.1 Thermal Accelerometer

Thermal accelerometers use the displacement of a hot air bubble to sense acceleration. The bubble, or more accurately, a temperature gradient in a gas, is created by passing electrical current through a thin metal wire that is suspended over a gas-filled cavity, acting as a heater. Additional wires are placed on either side of the heater at equal distances, which act as thermometers. This way, an acceleration reading for the direction perpendicular to the wires can be derived from the difference in temperature between the two thermometers: In case of no acceleration, both will be at the same temperature. However, due to the lower density of the heated air, an acceleration will cause the hot bubble to shift and the temperature distribution to become asymmetric, making one thermometer hotter than the other and causing a measurable difference.

A crucial advantage of thermal accelerometers over traditional mass-and-spring based MEMS designs is their high shock survivability and high dynamic range. There are no mechanically movable parts that can become compromised by impact or stiction when undergoing extreme accelerations on the order of several 10,000 g, since the hot air bubble serves as the proof mass and as such is essentially indestructible. Further, numerical simulations predict a scaling between acceleration and temperature difference that would even allow for reliably sensing these ultra-high accelerations.

One of the main challenges of this design lies at the lower end of the range: To be able to sense accelerations on the order of 0.001 g, the thermistors need to be able to measure temperature differences well below 0.001 °C. Their resolution limit is in large part determined by the material's electronic and thermal properties, which shall therefore be optimized.

1.2 Thermistor Figure of Merit

Thermistors allow measuring temperature through changes in resistance. The change in resistance of a material depends on its temperature coefficient of resistivity (TCR), which is defined as

$$\text{TCR} = \frac{1}{\rho} \frac{d\rho}{dT} \quad [\text{ppm}/^{\circ}\text{C}]$$

where rho and T are resistivity and temperature, respectively.

However, resistance also varies due to noise and resistivity fluctuations over time. The latter are usually more significant and can be characterized by the resistivity stability, defined as

$$\text{Resistivity Stability} = \frac{\Delta\rho}{\rho} \quad [\text{ppm}]$$

The minimum temperature that can be reliably sensed is then given by

$$T_{\min} = \frac{\text{Resistivity Stability}}{\text{TCR}} \quad [^{\circ}\text{C}]$$

This is the key figure of merit for films to be used in the thermal accelerometer.

Experimentally, measuring TCR requires extensive testing as explained in section 3.5, however it is possible to relate the TCR to overall resistivity, which can be measured much more easily and reliably. According to Matheissen's rule, the overall resistivity is made up of the contributions from phonon scattering in the lattice ρ_l , and from defects in the film ρ_d , where the former depends on temperature and the latter does not:

$$\rho = \rho_l(T) + \rho_d$$

If the material is sufficiently pure, i.e. does not have a significant fraction of foreign atoms incorporated into it due to e.g. oxidation during growth, one can assume that $d\rho_l/dT$ is the same for all films, and therefore $d\rho/dT$ is the same for all films. Under this assumption, the temperature resolution is then proportional to the absolute value of the resistivity variation, which can be taken as a simplified figure of merit.

Another good indicator of film quality would be the overall resistivity itself, as a value close to the bulk resistivity indicates the film has few defects that could cause fluctuations in resistivity.

1.3 Advantages of Sputtering

Using the resistivity as the film quality metric, one can compare the most common deposition methods for platinum films – evaporation, sputtering and ALD – when deposited using standard, non-optimized recipes, which is shown in Table 1.3.1. Sputtering performs the worst in this comparison; the reason why it was chosen as the method to optimize in this work is due to its high tunability. Table 1.3.2 compares the deposition methods by available process parameters. At four continuous and one binary variable, sputtering is much more customizable than its alternatives, making a significant improvement in film quality from adjusting the recipe parameters much more attainable.

Bulk Value	ALD	e-beam Evaporation	Sputtering
10.4 $\mu\Omega\cdot\text{cm}$	14 $\mu\Omega\cdot\text{cm}$	17 $\mu\Omega\cdot\text{cm}$	20 $\mu\Omega\cdot\text{cm}$

Table 1.3.1. Typical resistivity of platinum thin films deposited with different methods using standard, non-optimized recipes.

ALD	e-beam Evaporation	Sputtering
Temperature [$^{\circ}\text{C}$]	Beam Current [mA]	Power [W]
Exposure Mode (?)	Sweep Speed (?)	Pressure [mTorr]
		Temperature [$^{\circ}\text{C}$]
		Substrate Bias [V]
		DC vs. RF Power

Table 1.3.2. Available process parameters for common metal thin-film deposition methods.

2. Deposition and Patterning

2.1 Experimental Approach

The extensive tunability of sputtering also poses an experimental challenge in having to optimize a huge 4 ½-dimensional parameter space. To achieve this with a reasonable number of depositions, we chose a design-of-experiments (DOE) approach, assisted by the JMP software. For each available parameter two discrete values are chosen, low (-) and high (+), and then several combinations of low and high values are fabricated and characterized, in order to extract trends as to the influence of each parameter. For this to give meaningful results, it is important to make reasonable choices for each parameter's low and high values – if chosen too close together, the parameter's effects might not become apparent; on the other hand they might get overshadowed by second-order effects if the values are too extreme. Therefore some initial testing was done to find appropriate parameters.

Pressure

The lowest pressure that can be used is limited by the ability to sustain a plasma. Testing showed this threshold for DC plasma to be at 1.6 mTorr. For RF, no plasma extinguish was observed even at 1.4 mTorr, which is the lowest pressure that the turbo pump can achieve at 50 sccm Ar flow. To have some margin for fluctuations, the low pressure DOE value for both DC and RF was chosen to be 2 mTorr.

From literature and past experience it is known that a sputtering pressure of 75 mTorr or above results in porous platinum films, which is undesirable for the thermal accelerometer application due to mechanical reasons, so the high power DOE value was placed significantly below this level, at 30 mTorr.

Power

The highest power a target can be sputtered at without sustaining damage depends mostly on the material and target diameter, but many other parameters also play a role, including target thickness, bonding and backing plate material (if applicable), cooling water flow, gun and magnet type, clamping pressure and power type. Therefore it needs to be individually tested for each target and power type. A relatively safe method of finding a target's limit without damaging it is by monitoring the voltage as measured by the power supply. Starting at a known safe power level, the power is increased in small (5-10 W) steps, and at each step the voltage is monitored while the power is held constant for several minutes. If the voltage starts to rise continuously, or as an earlier warning sign, fluctuate strongly, this indicates the limit has been exceeded or almost reached. (Upon reaching the voltage rise point, the power must be decreased immediately – within seconds – to avoid target damage!)

Using this method, it was found that the platinum target voltage becomes unstable at ~315 W for DC power and ~180 W for RF power. To have safety margins for e.g. variable clamping pressure from different mounting, the high power levels were chosen as 280 W for DC and 160 W for RF. Reducing these values by 4x lead to the low power values of 70 W for DC and 40 W for RF.

Substrate Bias

A review of literature indicated that there is a sweet spot for substrate bias between 100-150V – significantly below this, its effects become diminished and significantly above, detrimental effects like increased surface roughness and decreased deposition rate become excessive. The biasing power supply on the Lesker-Sputter is controlled by setting the power; it was found that a power of 40 W results in about 125 V of bias, so this was chosen as the high DOE value and no bias as the low.

Temperature

The Lesker-Sputter is able to heat the substrate to a maximum temperature of 800 C. Initial tests were carried out at 600 C. Heating to this temperature was found to significantly worsen the base pressure in the main chamber, from 9E-8 Torr to 3E-5 Torr, which subsequently resulted in an oxidized film, as was confirmed by X-ray Photoelectron Spectroscopy (XPS), which showed 15% oxygen content in the film, even after removal of the upper atomic layers through in-situ sputter etching. After reducing the temperature to 400 C, oxidation was found to no longer be an issue, however when using a blank silicon wafer, XPS showed that a film of platinum silicide (PtSi) instead of platinum had been formed. Ultimately, the temperature was reduced to 270 C, which is identical to the default temperature of the standard ALD platinum recipe. This was found to be a usable high DOE value, and no heating as the low value.

An overview of all DOE deposition parameters is shown in Table 2.1.1. The 12 tested parameter sets, chosen with the help of the JMP software, are shown in Table 2.1.2. For each parameter set, two depositions were done: The first with a constant deposition time in order to determine the deposition rate, and the second, using this rate, aiming at a thickness of 30 nm. A thickness of 30 nm provides a good baseline for testing, as it is above the electron mean free path in platinum of 22 nm, such that the film's properties are not dominated by surface scattering, but is also thin enough to allow comparison to ALD and not waste material.

	Low	High
Power	70 W DC, 40 W RF	270 W DC, 160 W RF
Pressure	2 mTorr	30 mTorr
Temperature	no heating	270 C
Substrate Bias	no bias	40 W

Table 2.1.1. Overview of parameter values used in DOE.

DOE Number	1	2	3	4	5	6	7	8	9	10	11	12
Power Type	DC	DC	DC	DC	DC	DC	RF	RF	RF	RF	RF	RF
Power	-	-	-	+	+	+	-	-	-	+	+	+
Pressure	-	-	+	-	+	+	-	-	+	-	+	+
Temperature	-	+	+	+	-	-	-	-	+	-	+	+
Substrate Bias	-	+	+	-	-	+	-	+	-	+	+	-

Table 2.1.2. Parameter sets used in DOE.

2.2 Recipe Writing on Lesker-Sputter

While the Lesker-Sputter has many tunable parameters, the standard recipes written for the tool do not incorporate the use of the full set of these parameters. The standard DC and RF recipes written for each source allow the user to easily set the source power, chamber pressure, and deposition time at the start of the recipe. Once these recipes are running, the user can manually change these and other parameters, including the substrate bias and temperature. However careful timing is required to make these manual changes, as attempting to make these changes in many stages of a running recipe can trigger interlock errors. Additionally, manually tuning the recipe while it is running requires additional effort on the part of the tool operator. To address these limitations, users can create their own recipes for the Lesker-Sputter. Recipes can be written such that all the parameters a user wants to directly control can be set in the user-set values box that appears when a recipe is loaded.

The most important point to remember when writing recipes for the Lesker-Sputter is that making changes to a recipe that already exists will implement those changes on every instance where that recipe is called. The master recipes that exist for each source are a compilation of sub-recipes, as can be seen by clicking the View Recipe

button within the Recipe Editor tab. Recipes are only editable if the “Edit Disable” box next to the recipe is not checked. The easiest way to create a new recipe is to start by making a copy of a similar recipe that already exists. To do this, click the Recipe Editor tab, open the recipe to be copied, click the copy button in the upper right, and rename this copy with the desired new recipe name. Again, any changes made to the sub-recipes in the copy will change these sub-recipes in every recipe in which they are called. Therefore it is vital that these sub-recipes are not changed. To make changes to the sub-recipes, create and rename copies of those recipes. To give us full control of substrate temperature and substrate bias, and to ensure we had the proper pressure and gas flows required to strike the plasma for low-pressure depositions, we created our “E241 Ultimate Master Recipe” (Figure 2.2.1). Below is a description of each of the parameters we added to our recipe and an explanation of how to add these parameters when creating a new recipe.

Drag	Step	Equipment Type	Equipment Name	Equipment Operation
↕	1	Recipe	Set Abort Recipe	Abort Process
↕	2	Recipe	Run Recipe	E241 Substrate Heat Two Ste...
↕	3	Recipe	Run Recipe	Platen Motor Rotate 20 RPM
↕	4	Recipe	Run Recipe	E241 Downstream Control X ...
↕	5	Recipe	Run Recipe	PS4 Plasma Ignition
↕	6	Recipe	Run Recipe	E241 PS4 Ramp To Power an...
↕	7	Recipe	Run Recipe	PS2 Plasma Ignition- Src3
↕	8	Recipe	Run Recipe	E241 Downstream Control R...
↕	9	Recipe	Run Recipe	PS2 Ramp To Power and Bur...
↕	10	Recipe	Run Recipe	Source 3 Deposition Time - U...
↕	11	Recipe	Run Recipe	PS2 Plasma Extinguish
↕	12	Recipe	Run Recipe	PS4 Plasma Extinguish
↕	13	Recipe	Run Recipe	Substrate Heat Turn Off
↕	14	Recipe	Run Recipe	Downstream Control Turn Off ...
↕	15	Recipe	Run Recipe	Platen Motor Stop

Figure 2.2.1. E241 DC Source 3 Ultimate Master Recipe.

Substrate Heating

To add substrate heating to a custom recipe, add the “Substrate Heat – User Set Value” recipe to the new master recipe. Add this step to the beginning of the recipe, just after the Abort Process step. The “Substrate Heat Turn Off” recipe should also be added near the end of the recipe, right after the plasma(s) have been extinguished. The standard “Substrate Heat – User Set Value” recipe for substrate heating includes a wait clause to ensure the heater temperature is within 3°C of the desired temperature before the recipe is allowed to continue. In this recipe the ramp rate for the temperature is set at 10°C/sec. Both of these parameters can be changed (only if a separate copy is made!). To change the ramp rate, click on the ‘-R’ button located on

the far right in the 'Config' column. Note that setting a faster the ramp rate can result in overshoot of the desired temperature point. To initially heat at a faster rate and also limit overshoot, we created a version of this recipe with two ramp phases. The first phase has a fast ramp and is active until the temperature is within 30°C of the desired set point. The second phase has a slower rate and is active until the temperature is within 3°C of the target temperature. The Lesker-Sputter does not have active cooling, so it takes a while for the substrate to cool back down. This can be important in making sure the substrate is at a reasonable temperature for the next user, especially since most users do not know to check what the substrate temperature is before beginning their deposition.

Substrate Bias

Substrate bias can be added by adding the necessary steps for PS4. The "PS4 Plasma Ignition" and "PS4 Ramp To Power and Burn In" recipes should be added to the recipe prior to the steps for igniting the main plasma. The "PS4 Extinguish" recipe is added immediately before or after the main plasma is extinguished. To tune parameters within these recipes, be sure to first create a copy.

Pressure and Gas Flow for Striking the Plasma

For low-pressure depositions, the pressure and gas flows may need to be raised in order to get the plasma to strike. As with the other parameters above, this can be done in the existing master recipes by manually changing the pressure and gas flow values in the Deposition window at the right time while the recipe is running. Alternately, these changes can be added as steps in a new recipe, so they will happen automatically when the recipe is run. We accomplished this by creating our own versions of the "Downstream Control Reduce to X mTorr" recipe. The first version, which set higher pressures and gas flows, is located upstream of the plasma ignition steps. The second version, which set the pressure and gas flow desired for the deposition, is located after the plasma ignition steps.

After we created our ultimate master recipe that was capable of tuning all of the parameters described above, we wanted to modify it for the cases in which we did not want to set certain parameters. This was relevant for cases in which we wanted a room temperature deposition and thus did not want to set the substrate temperature. It was also relevant for cases in which we did not want to apply a substrate bias. While it is possible to set the value for the substrate bias at zero, doing so actually causes errors during the recipe when one of the plasma checks cannot be met. This can be addressed manually by clicking the skip button when it reaches the step where the recipe gets stuck, or by explicitly skipping that step in the recipe. To do this, access the recipe in the Recipe Editor and click on the Skip box (on the right) for the steps

that should be skipped. Our “E241 Ultimate Master Recipe” is available as a recipe on the Lesker-Sputter for use and as an example of how to add all the parameters discussed here to a recipe.

2.3 System Debugging on Lesker-Sputter

The Lesker-Sputter has some bugs associated with using the substrate bias and heating. Plasma flickering was observed when using the substrate bias. This flickering is a result of the brushes, which provide contact to the rotating substrate holder, briefly losing contact. To avoid this, the stage can be lowered by 2-3 turns. There are several things to be aware of if the stage is lowered. First, lowering the stage may change the deposition rate since this changes the distance from the wafer to the target. This should not be a problem as the deposition rate will not be characterized at the fully-raised stage height for depositions with a non-zero substrate bias, but it is something to be aware of. Additionally, the substrate temperature will not match the desired set point if the stage is lowered. When the stage is lowered the substrate holder is not in direct contact with the heating element and thus will not be at the heater temperature. This may not be as much of an issue for short depositions, but it could cause deviations in the substrate temperature from the desired temperature as the deposition time increases.

The other issue to be aware of is the stability of the substrate heating temperature. The controller for the substrate does not do a particularly good job of maintaining the desired substrate temperature, in part because there is no active cooling. During our depositions, we noticed the actual temperature could be more than 12°C above the desired temperature. This temperature overshoot did not appear to be limited to an initial overshoot as it was also observed more than ten minutes into the deposition. We did not devise a solution for these temperature fluctuations, but trying to tune the heater controller may improve these fluctuations.

2.4 Platinum Etching

Due to its chemical inertness as a noble metal, platinum is known to be a difficult material to etch. Therefore the probably most common way of patterning it is by liftoff. This was however not an option for this project, as half of the depositions are carried out at 270 C, well above temperatures that photoresist can withstand without burning or blistering (~150 C).

Reactive ion etching of platinum is not allowed in the plasma metal etchers in SNF, as the platinum does not form volatile compounds with the etchant gases, so there could be significant redeposition of conductive material inside the etch chamber which can cause damage to tools not specifically designed for this. The only dry etching option is therefore ion milling, which has been tested before and been found to work

reasonably well, but has several disadvantages, such as poor selectivity and damage to underlying layers, plasma damage and hardening of resist, and redeposition of platinum on resist sidewalls, which remains even after resist removal, as shown in Figure 2.4.1.

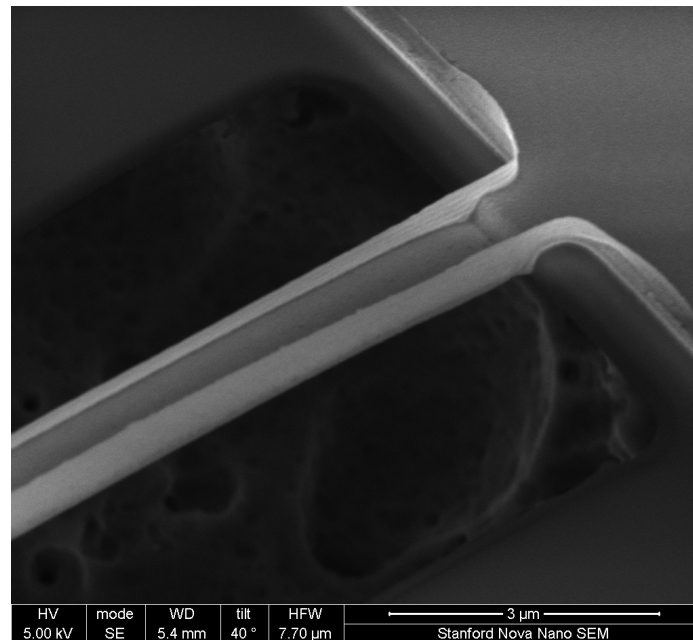


Figure 2.4.1. Suspended platinum beam patterned by ion milling, with vertical beads caused by redeposition of platinum on the photoresist sidewall.

Wet etching was explored as an alternative option to potentially address these issues. The only liquid etchant known to have a significant etch rate for platinum is aqua regia. To improve selectivity against photoresist, dilute aqua regia, i.e. a 3:1:2 mixture of $\text{HCl}:\text{HNO}_3:\text{H}_2\text{O}$, is most commonly used. Literature reports an etch rate of 3.5 nm/min for platinum and close to zero for silicon or silicon dioxide, i.e. excellent selectivity against the two most common underlying layers.

In our testing however, dilute aqua regia showed no effect on lithographically patterned 30 nm thick sputtered platinum films, even after being submerged for over 30 minutes, except in areas of the wafer that had been scratched by tweezers. The most likely explanation for this is surface passivation, which can be addressed by an argon sputter etch or an HF dip. The latter was successfully tested; after a 30 second dip in 50:1 HF, etching of the platinum layer was observed, although at an about 2x slower rate than expected. More significantly, the etch was found to cause an excessive undercut, completely removing all features below 10 μm, even when being timed to only etch a few 10s of nm in depth. This makes it entirely unusable for patterning thermistors to be used in a thermal accelerometer, therefore for the purposes of this study, all patterning of characterization wafers was done using ion milling as described above.

3. Characterization

3.1 Thickness Measurements on Thin Metal Films

The most common way in SNF of measuring the thickness of metal films deposited by evaporation or sputtering used to be to perform a step-height measurement with a stylus-based profilometer. However for fairly thin films of only a few 10s of nm, this does not provide very high accuracy, mostly due to the noise floor from mechanical vibrations. For this reason, many users switched to using 3D optical profilometry instead when the Taylor-Hobson CCI-HD tool was installed, which was able to measure much smaller steps, having a nominal resolution of 0.1Å in the z-direction. The CCI-HD has since been replaced by the Sensofar s-neox, which among other methods can also perform the same type of interferometry-based measurement as the CCI-HD.

Therefore this was the initially planned way of thickness measurement for this study. Unfortunately, unlike formerly on the CCI-HD, performing this measurement on the s-neox was found to suffer from poor repeatability and high variability even for steps very close to each other, as shown in Figure 3.1.1. This issue mostly disappeared at thicknesses above 100 nm, but still affected too many of the rate characterization wafers to be a viable method overall.

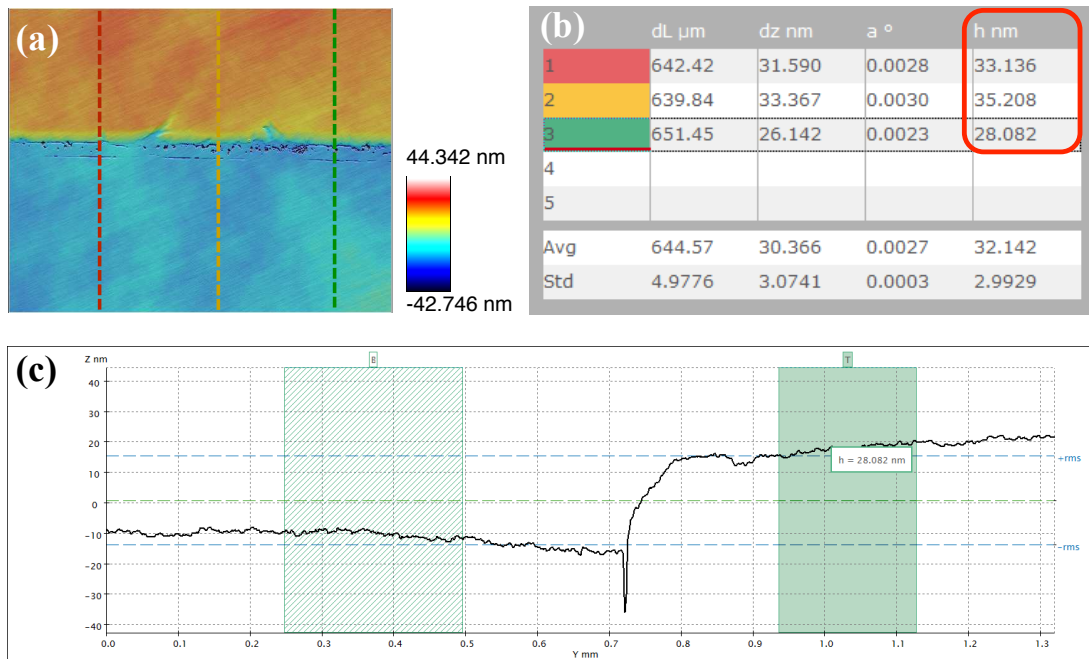


Figure 3.1.1. Step height measurement of a ~30 nm thick Pt film with 3D optical profilometry using the Sensofar s-neox. (a) 2D height profile with dotted lines indicating the 1D profiles used. (b) Measurement results of the 1D profiles, colors in the left column corresponding to the dotted lines in the 2D image; step heights marked in red. (c) 1D profile from the green dotted line with automatically chosen step height areas marked.

As an alternative, other methods were explored. Profilometry using the KLA Tencor Alpha Step D-100 in the Nanopatterning Cleanroom at SNSF proved to be more accurate than the s-neox for films below 100 nm, but as to be expected, was also limited at thicknesses below 30 nm, even after extensively optimizing all measurement parameters such as scan speed, length, stylus force and averaging.

Another surface scanning method, with a much higher vertical resolution up to atomic lengthscale, is Atomic Force Microscopy (AFM), which was tested using a JEOL AFM in the Nanoscale Prototyping Laboratory (Prinz Lab). Despite its high resolution, it was found to be entirely unreliable for the purposes of step height measurement, mostly because the scan area is limited to a maximum of 25x25 μm , inside of which it is hard to find level surfaces on either side of the step, since the steps don't actually resemble perfect step functions, but usually have beads and areas slowly changing in height on either side of the border.

The most universally applicable method was found to be X-ray Reflectivity (XRR), which works well in the range from 5 to 100 nm and is described in more detail in section 3.2.

For extremely thin films even out of range for XRR, optical methods, in particular spectral reflectance and ellipsometry, using the tools FilMetrics F20 in the Nanopatterning Cleanroom and J.A. Woollam M2000 in SNF, respectively, proved to give good fits and very reliable results. Naturally, they are limited to film thicknesses below the optical penetration depth of the material, which is around 12 nm for platinum.

An overview of the tested methods and their advantages and disadvantages is given in Table 3.1.1.

3.2 X-ray Reflectivity (XRR)

X-ray reflectivity (XRR) is a technique used to characterize the properties of thin single layer and multilayered films. The film parameters it can determine are thickness, density, and surface or interfacial roughness (Figure 3.2.1). For example, Figure 3.2.2 shows that wafer 1 is thicker than wafer 5 because the width of the fringes is narrower. Using this technique, each film's properties were measured. Figure 3.2.3 shows the XRR data of platinum deposited on thermally grown SiO₂.

Although most of the sputtered film's thicknesses were measured with XRR, the technique has its limitations to what it can measure. First, XRR had issues when the film was so rough that its roughness was comparable to its thickness. Normally, the width of the fringes is used to fit the thickness. However the fringes go away when film is rough, making it impossible to obtain the thickness data from the measurement (Figure 3.2.4). Fitting density is another issue. For the XRR measurement, the critical angle increases with density. With fringe amplitude sometimes affecting the density

Method	3D Optical Profilometry	Stylus Profilometry	Atomic Force Microscopy	X-ray Reflectivity	Spectral Reflectance	Ellipsometry
Tool	Sensofar s-neox	KLA Tencor Alpha Step D-100	JEOL JSPM-5200	PANalytical X'Pert	FilMetrics F20	J.A. Woollam M2000
Accessibility	+ fast, cheap	+ fast, cheap	- very slow	- slow, pricey	+ fast, cheap	+ fast
Surface Impact	+ non-contact	- sample contact	- sample contact	+ non-contact	+ non-contact	+ non-contact
High Temperature Compatibility	- low temperature only, needs Kapton tape	- low temperature only, needs Kapton tape	- low temperature only, needs Kapton tape	+ high temperature possible, no Kapton tape	+ high temperature possible, no Kapton tape	+ high temperature possible, no Kapton tape
Limitations	- unreliable below 100 nm	- unreliable below 30 nm	- always unreliable	- unreliable below 5 nm and above 100 nm	- fails above 12 nm	- fails above 12 nm
Other				- affected by roughness		+ higher accuracy vs. Spectral Reflectance

Table 3.1.1. Comparison of various methods for measuring the thickness of thin metal films.

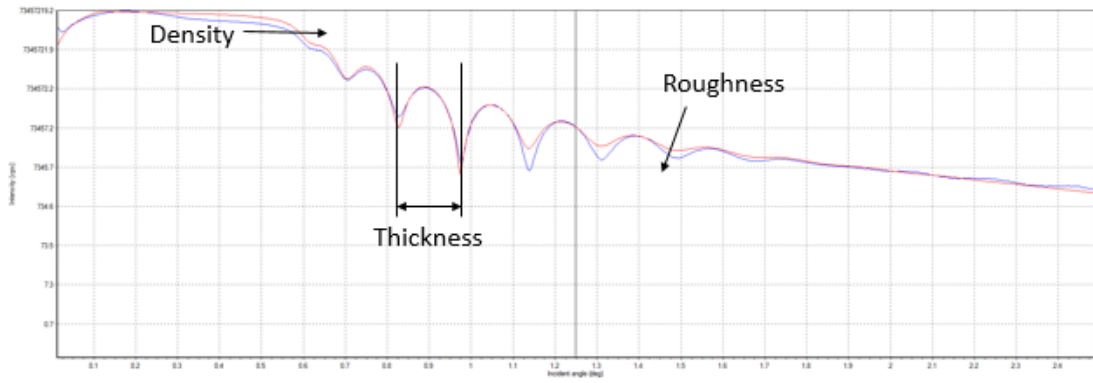


Figure 3.2.1. Typical X-ray reflectivity data (blue) with fit (red).

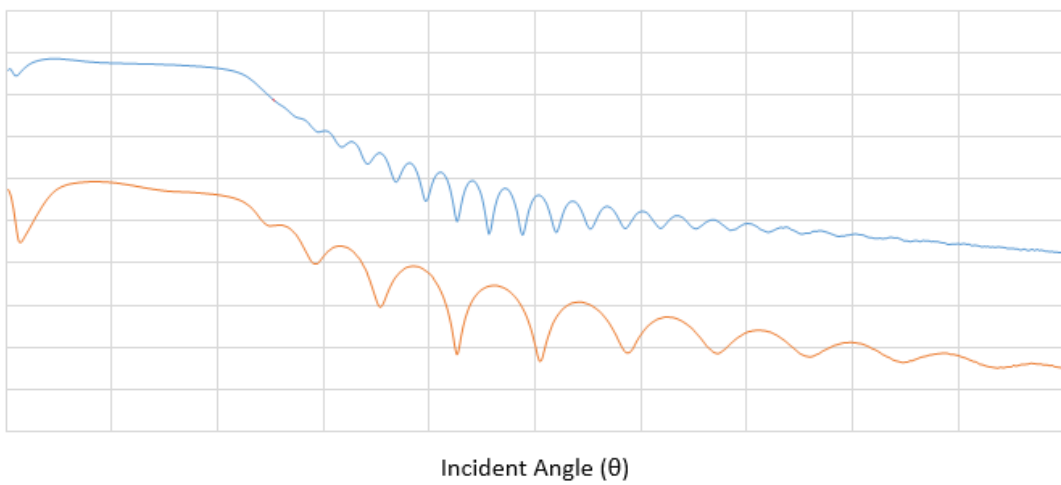


Figure 3.2.2. X-ray reflectivity of platinum on a thermally grown SiO₂ (192nm)/Si substrate (blue line – wafer 1, orange line – wafer 5).

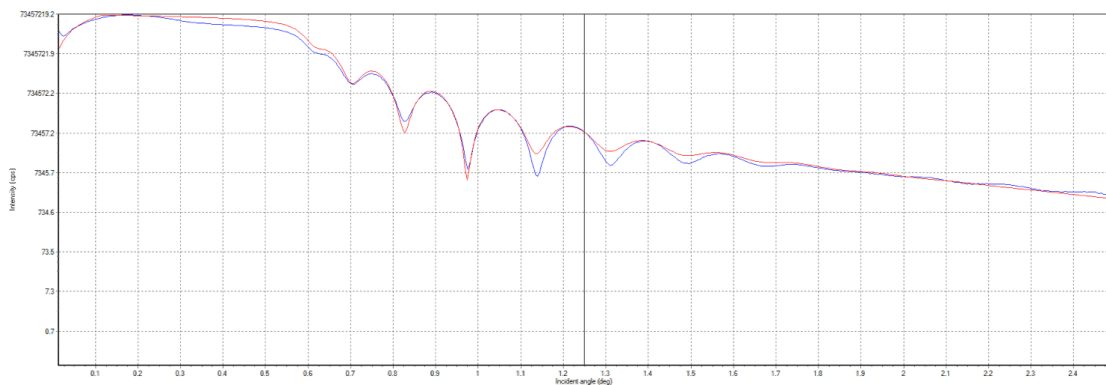


Figure 3.2.3. X-ray reflectivity of platinum on a thermally grown SiO₂ (192nm)/Si substrate showing film thickness and density fitted data (blue: Measured data, red: fitted).

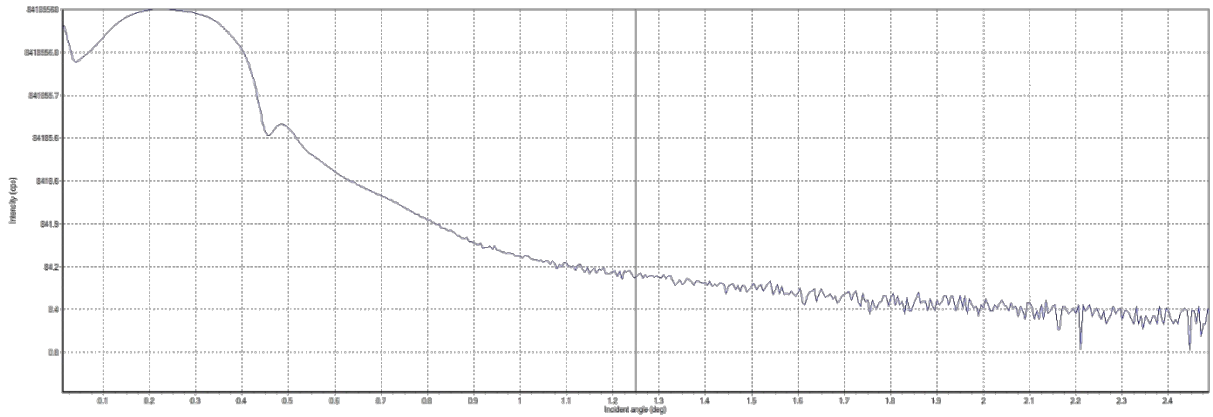


Figure 3.2.4. X-ray reflectivity of platinum on a thermally grown SiO₂ (192nm)/Si substrate for a rough film, where there are no fringes to fit.

and having multilayered structure (Si/SiO₂/Pt), it is hard to get an accurate fit for both density and thickness.

3.3 X-ray Powder Diffraction (XRD)

Non-symmetric and symmetric x-ray powder diffraction (XRD) measurements were done on the sputtered films. Non-symmetric measurements give information about the crystallinity of the deposited films while the symmetric measurement, known as a theta-2theta measurement, provides information on the in-plane grain size, quantitative crystal orientation, phase ID and lattice parameter. Figure 3.3.1 illustrates the difference between non-symmetric and symmetric measurements. From the symmetric measurement, we anticipated correlating the grain size and crystal orientation to the electrical properties of sputtered platinum.

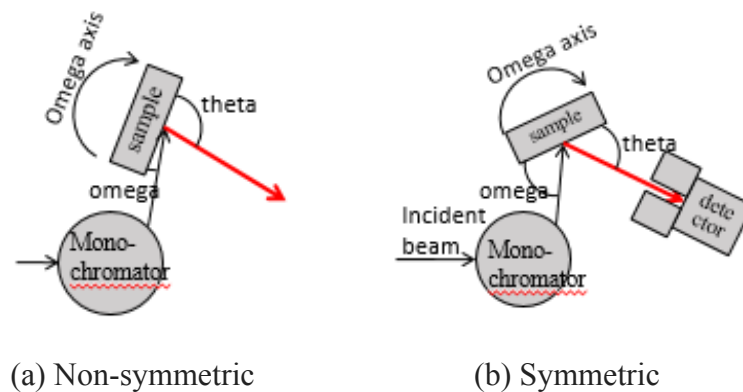


Figure 3.3.1 (a) Non-symmetric versus (b) symmetric XRD measurements.

3.3.1 Non-symmetric measurement (2theta scan, glazing incidence)

From the non-symmetric scans, it was observed that all of our sputtered films were crystalline. Three of the major platinum peaks, (111) at 39.76° , (200) at 46.24° and (220) at 67.45° were observed. (Figure 3.3.1.1)

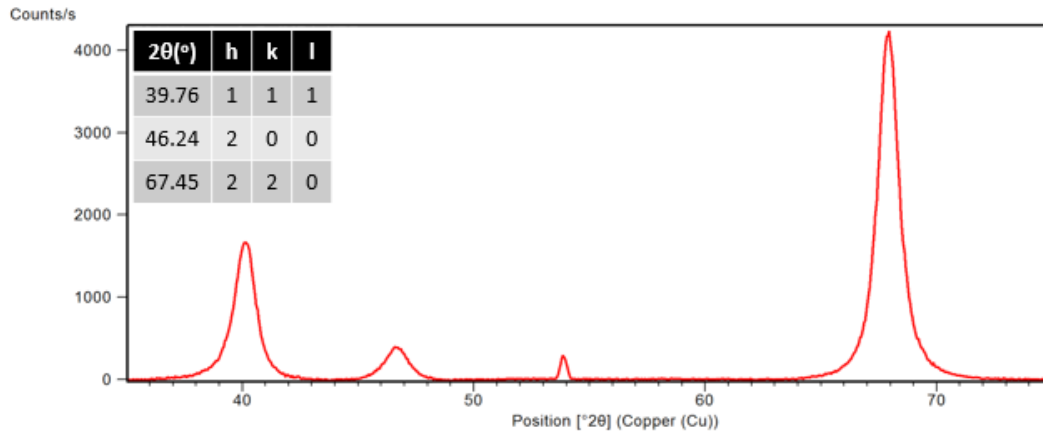


Figure 3.3.1.1. 2theta measurement of platinum on a thermally grown SiO₂ (192nm)/Si substrate.

3.3.2 Symmetric measurement (Theta-2theta scan)

In order to obtain information about grain size and quantitative crystal orientation, a theta-2theta scan was conducted. On the linear scale plot none of the platinum peaks were observed. (Figure 3.3.2.1) The peak observed near 69° is a Si(400) peak from the Si(100) substrate. If we zoom into the 35° to 55° region, we can see the platinum peaks which have peaks with 7 orders of magnitude fewer counts than the silicon (Figure 3.3.2.2). When a background noise subtraction algorithm was applied, all the platinum peaks went away. There are two reasons why the platinum peaks are weak compared to the peak from the silicon substrate. First, unlike for the non-symmetric scan, in the symmetric scan the incident beam penetrates deep into the sample. Therefore since the platinum film is only around 30nm thick and the substrate is about 0.5mm, there are much stronger signals coming from the substrate. Also, the silicon peak is sharper than the platinum peak. Since the silicon substrate is a single crystal there is less peak broadening, whereas for polycrystalline platinum the peak is subjected to peak broadening. This broadening of the platinum peak results in a lower peak count than would be present were it single crystalline, further burying the platinum signal.

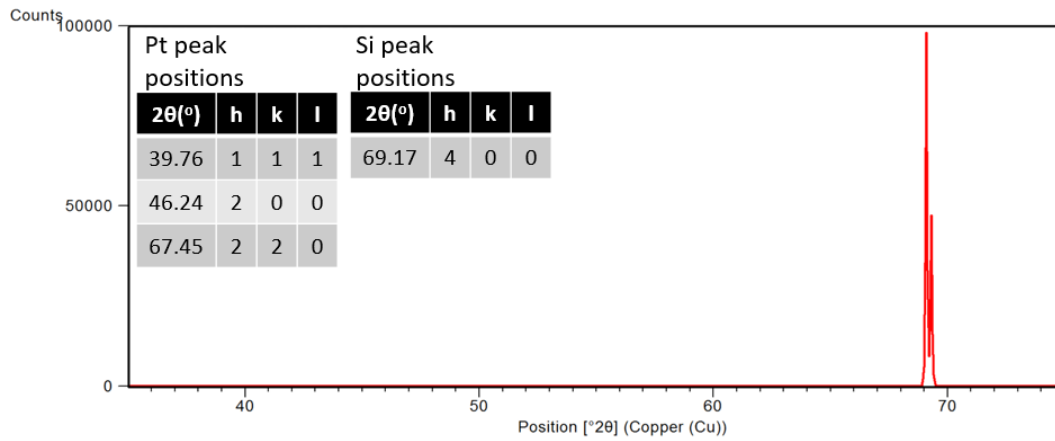


Figure 3.3.2.1. Theta-2theta measurement of platinum on a thermally grown SiO₂ (192nm)/Si substrate.

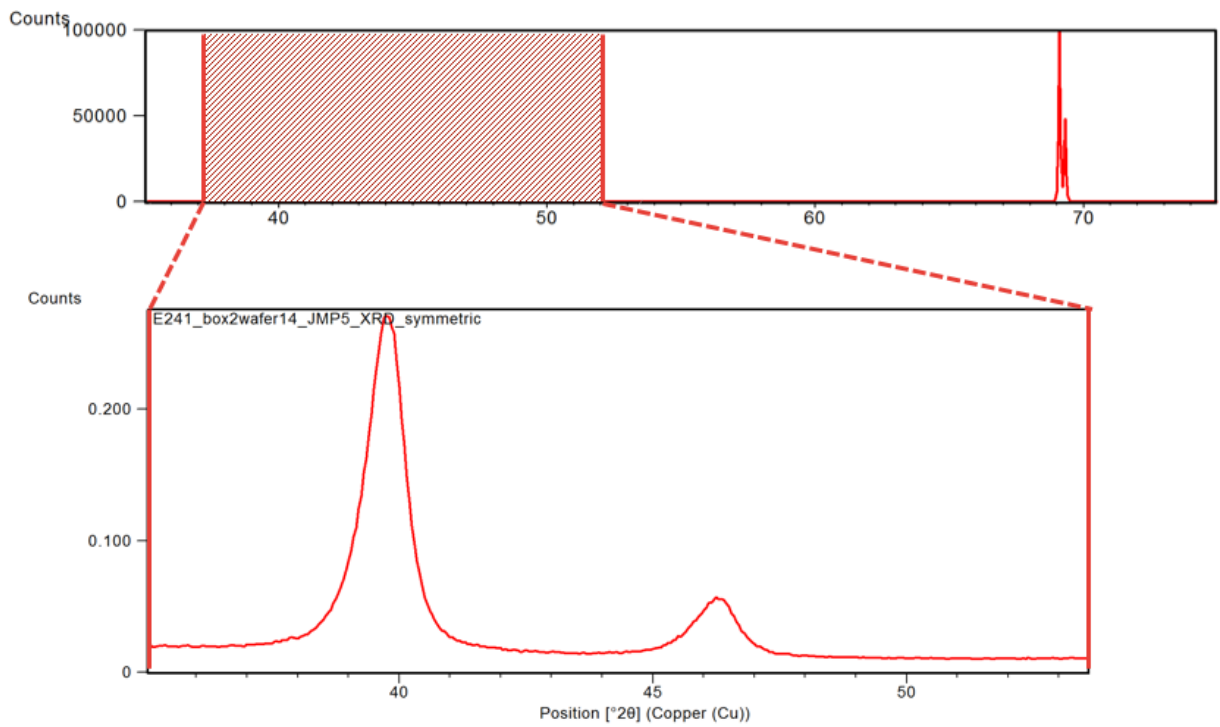


Figure 3.3.2.2. Theta-2theta measurement of platinum on a thermally grown SiO₂ (192nm)/Si substrate.

3.4 Room-Temperature Electrical Measurements

To allow for electrical measurements, the wafers were lithographically patterned with four-point probe structures from an existing mask set, mostly consisting of long, narrow beams ranging in width from 0.5 to 10 μm and in length from 1000 to 8080

um. This is comparable to the dimensions used in the thermal accelerometer, except with a wider range and larger number of variations, and with bondpads on the same layer, making it ideal for the purposes of this study.

Resistivity at room temperature was measured by contacting these structures with the cascade probe station in Allen 155A. The resistance for individual beams was calculated from IV-sweeps carried out with the connected Keithley 4200 SMUs. Resistivity was then calculated using the known beam dimensions and film thickness measured by XRR. Initial testing found the results not to depend strongly on the current density used. All later tests were then carried out with the upper range of current in the IV sweep set to $1\text{E}5\text{ A/cm}^2$. This is realistic level for use in the thermal accelerometer, as damage from electromigration can occur above $1\text{E}7\text{ A/cm}^2$ and suspended beams start to fail from thermal overload above $2\text{E}6\text{ A/cm}^2$.

The results for resistivity were found to depend significantly on the beam width measured, with narrower widths giving lower results, in some cases even below the bulk resistivity value for platinum. This can likely be explained by two causes: One, during lithography the beams were deliberately underexposed slightly in order to increase the yield and avoid broken lines considering their excessive length, and this probably also had the effect of making them slightly wider than designed for on the mask. In addition to that, some material will have redeposited on the resist sidewalls during ion milling as described in section 2.4, increasing the effective beam width further. One can however correct for this excessive width by introducing it as a fitting parameter when measuring multiple widths of the same beam, which ultimately resulted in very consistent results over various lengths and widths.

The second method employed to measure resistivity was by contacting an unpatterned area of the wafer with a 4-point probe head, using the prometrix resistivity mapping system in SNF. Several users have reported the prometrix to give unreliable results for very thin films, e.g. Pt films from ALD near the nucleation threshold. To test the repeatability, multiple measurements with the probe head at a slightly different location each time, were carried out for all wafers. The average standard deviation for each wafer's measurements was found to be 0.6%, indicating that repeatability is very good for films with thicknesses around 30 nm. Comparing the average resistivity from prometrix with the beam width-fitted results from cascade, there are significant differences only for the most resistive wafers, with a maximum of 8.7%, but there is very good agreement for most wafers with the median difference being 1.2%.

3.5 Temperature-Controlled Measurements

Film stability was measured using the same four-point probe structures described in the previous section. After scribing the wafer into dies, each containing several devices, the dies were silver pasted to a carrier. Several devices from each die were wirebonded to the carrier bond pads using aluminum wire (Figure 3.5.1). The setup

was placed in an oven and stabilized at 30°C. Prior to conducting stability tests, each structure was burned in at a current density of 5e6 A/cm² for 10 min. This initial burn in phase is important to relax the platinum film and work out any mobile defects in the film. Typically the resistance will decrease during the initial part of this phase, and burn in is considered complete when the film resistance has stabilized. After burn in, stability measurements were performed by measuring the resistance of each device approximately every second for a total of 30 minutes. The resistivity was calculated using the nominal beam dimensions, and the stability of each run was quantified by finding the average resistivity of each beam and then measuring the root mean square (RMS) deviation.

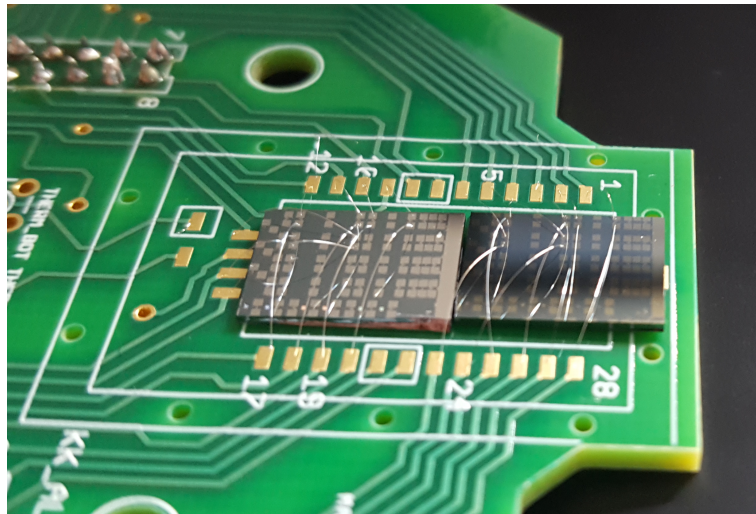


Figure 3.5.1. Dies from two different DOE wafers are attached to a carrier, and then devices from each wafer are wirebonded to the carrier bond pads.

Figure 3.5.2(a) shows the typical variation in resistivity seen for a stability run. Across all wafers, the resistivity stability varied from 7.2e-5 $\mu\Omega\cdot\text{cm}$ to 1.35e-3 $\mu\Omega\cdot\text{cm}$ (Table 4.1.1). The resistivity stability of the sputtered platinum films was generally comparable to the stability of a 9.46 nm thick ALD platinum film. DOE number 4 exhibited the best stability, with several other DOE wafers and the ALD film exhibiting only slightly higher RMS deviation than DOE number 4. These results indicate that certain deposition parameters do yield more stable films, and that sputtered films can be as stable as ALD films.

In addition to characterizing film stability, the temperature coefficient of resistance (TCR) was measured for a subset of the films. To measure the TCR, the oven temperature was stabilized for 25 minutes for temperatures ranging from 10°C to 50°C, in 5°C increments. At each temperature, an IV curve was collected for each beam and the beam resistance was determined by fitting this curve. The TCR was calculated from a linear fit of the resistance data as a function of temperature.

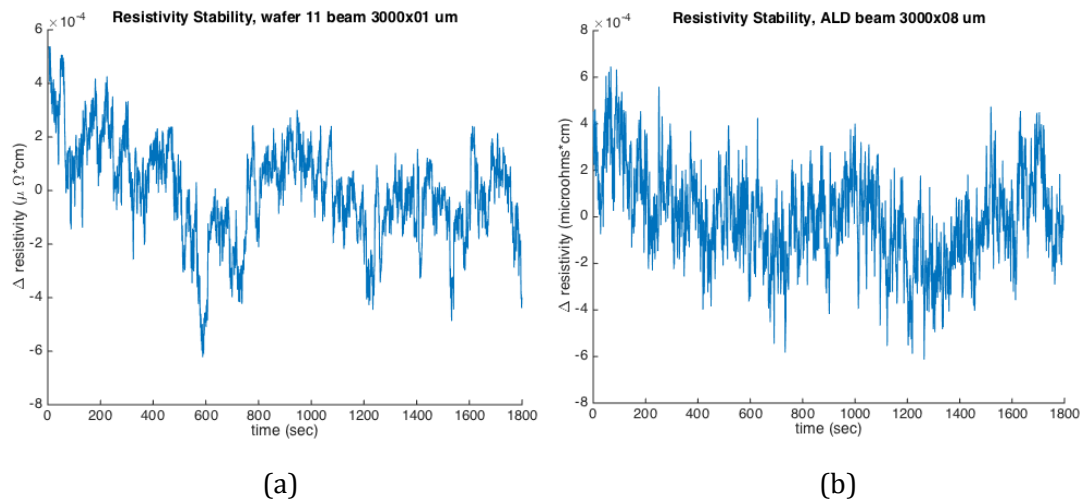


Figure 3.5.2. Resistivity stability for (a) a 3000 μm long, 1 μm wide sputtered platinum beam deposited with RF at high power, temperature, and substrate bias and low pressure and (b) an ALD platinum beam.

The results of the TCR tests show a range from $9.15\text{E-}4$ to $2.81\text{E-}3$ $1/^\circ\text{C}$ (Table 4.1.1). We can compare these values to that found for ALD platinum. The TCR of ALD platinum is $1.5\text{E-}3$ and $2.1\text{E-}3$ $1/^\circ\text{C}$ for film thicknesses of 50 nm and 20 nm, therefore we anticipate the TCR to be near $2\text{E-}3$ $1/^\circ\text{C}$ for a 30 nm film. Excluding DOE 5, the DOE sets exhibited a TCR similar to or better than the value found for ALD platinum. This suggests these films could provide better sensitivity to sense small temperature fluctuations.

4. Results and Outlook

4.1 DOE Results

A summary of the results from the DOE is listed in Table 4.1.1. Parameter set 8 was dropped due to an excessively low deposition rate.

There are very large differences in all measured properties, with e.g. the resistivity being 8x higher in the worst compared to the best wafer, indicating that the deposition parameters do indeed play a significant role.

Comparing the various figures of merit, it can be seen that they are somewhat but not entirely correlated. The wafer with the lowest resistivity, number 12, also has good, but not the best stability and TCR. In return, wafer 4, which shows the best stability, is only the 7th-lowest in resistivity. Wafer 5, with the highest resistivity, also has the lowest measured TCR, somewhat validating the assumption from section 1.2 that a high resistivity, large number of defects and low TCR would be correlated.

DOE Number	1	2	3	4	5	6	7	8	9	10	11	12
Power Type	DC	DC	DC	DC	DC	DC	RF	RF	RF	RF	RF	RF
Power	-	-	-	+	+	+	-	-	-	+	+	+
Pressure	-	-	+	-	+	+	-	-	+	-	+	+
Temperature	-	+	+	+	-	-	-	-	+	-	+	+
Substrate Bias	-	+	+	-	-	+	-	+	-	+	+	-
Deposition Rate [nm/min]	4.04	3.26	3.78	16.2	30.8	25.0	0.406	0.239	0.282	1.35	0.491	2.25
Resistivity (cascade) [$\mu\Omega\cdot\text{cm}$]	19.7	14.0	14.6	15.6	102.2	43.0	15.5	/	13.2	16.1	15.5	12.3
Resistivity (prometrix) [$\mu\Omega\cdot\text{cm}$]	19.6	13.8	14.5	15.6	94.1	41.6	15.3	/	13.1	15.9	14.7	12.1
Resistivity Stability [$\mu\Omega\cdot\text{cm RMS}$]	4.3E-4	1.3E-3	1.4E-3	7.2E-5	2.3E-4	1.4E-4	3.3E-4	/	4.2E-4	3.9E-4	1.9E-4	2.8E-4
TCR [$1/^\circ\text{C}$]	2.8E-3		2.7E-3		9.1E-4		2.0E-3	/	1.8E-3			2.3E-3

Table 4.1.1. Overview of DOE Results.

To determine the influence of each parameter individually, the results for resistivity were fed back into the JMP software in order to perform a least-squares analysis. The most significant parameters overall were found to be temperature and power type, with higher temperature and RF power giving better results. For the other parameters, it was necessary to perform two separate JMP analyses, considering only either the DC or RF cases, in order to gain meaningful insight. The results for the DC wafers (Figure 4.1.1) show that lower resistivity correlates with low power, low pressure and high bias, and as already expected, high temperature. Aside from temperature, the RF case (Figure 4.1.2) is almost completely reversed, preferring high power, high pressure and low bias.

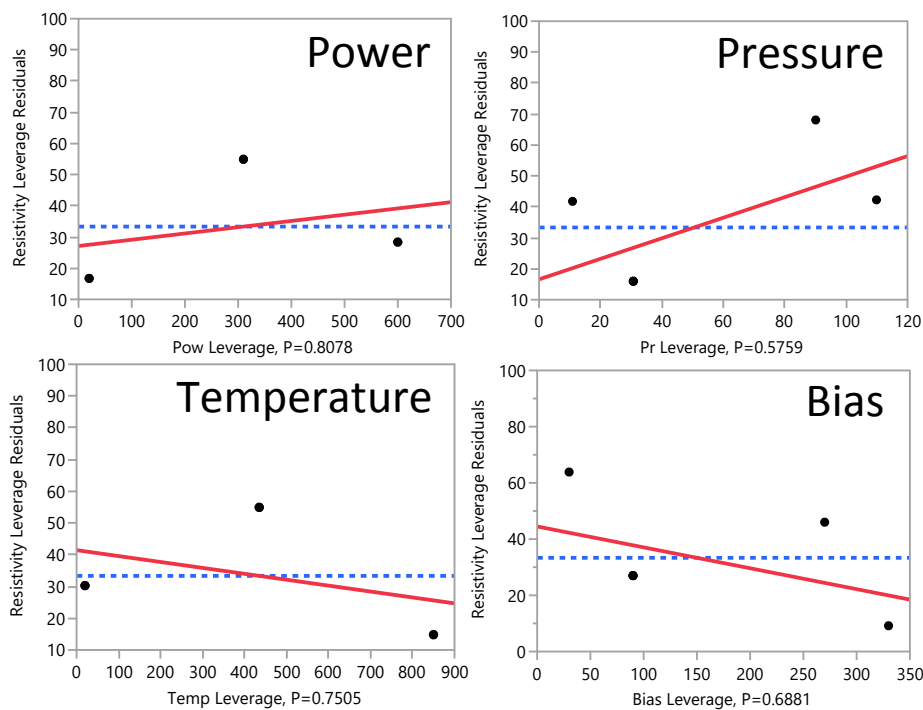


Figure 4.1.1. Analysis of parameter leverages on resistivity for DC sputtering.

4.2 Summary

Using a design-of-experiments analysis, the impact of various process parameters on the electrical characteristics of sputtered platinum films has successfully been characterized. It was possible to achieve a resistivity of $12.1 \mu\Omega \cdot \text{cm}$, which is significantly closer to the bulk value of $10.4 \mu\Omega \cdot \text{cm}$ than the best ALD films of comparable thickness fabricated to date ($14.1 \mu\Omega \cdot \text{cm}$). The resistivity stability could also be improved over ALD platinum, however using a different parameter set. On the basis of this work – also including the insight gained on characterization methods – it should be possible to further improve the characteristics of platinum films and outperform other deposition methods in every figure of merit by also quantitatively optimizing the sputtering parameters.

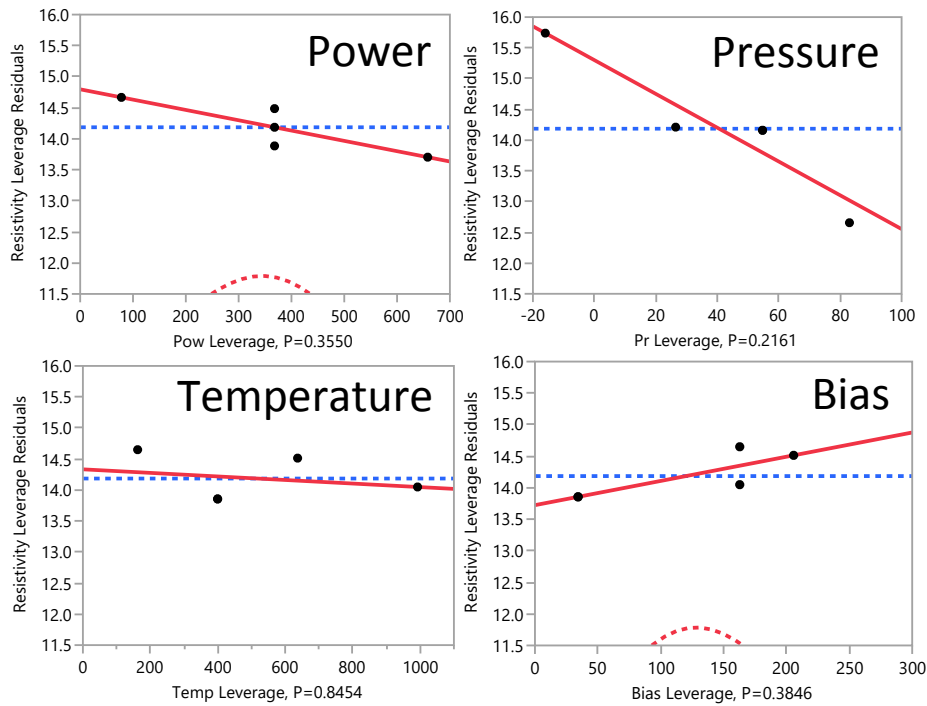


Figure 4.1.2. Analysis of parameter leverages on resistivity for RF sputtering.

4.3 Future Work

In order to better understand and quantify the variations in the material and electrical properties of the platinum films deposited under the full range of deposition conditions considered here, we aim to conduct additional deposition and characterization work. To accomplish this, we will perform more extensive iterations of the deposition parameters around the points in the parameter space deemed to be near optimal from these initial tests. These future depositions will use (111) Si wafers instead of the (100) Si used here. Because of the different crystal orientation of the (111) Si, the location of the silicon peaks on the symmetric XRD scans will be located at 28.42° , rather than the 69.17° location of (100) Si. This shifting of the silicon peak away from the location of the platinum peaks will enable us to acquire the desired XRD measurements for the platinum films, which we can then use to determine the grain size and quantitative crystal orientation.

We are additionally interested in testing the depositions on sapphire wafers. The lattice mismatch between sapphire and (111) Pt is only 0.6%. This represents a reduction in the lattice mismatch relative to that of either (100) Si or (111) Si, which will reduce the film and interface stresses. To improve the resistivity stability of the films, we will also test annealing methods for the platinum films. Based on the results of previous members of our lab, we anticipate a resistivity improvement on the order of 10% can be achieved even at short anneal times and low thermal budgets.

We further intend to test the integration of the optimal sputtered platinum films into our thermal accelerometer fabrication process. Incorporating these optimized films into our device provides the ideal opportunity for us to rigorously compare the quality of the sputtered films relative to ALD films for the purposes of our devices. Based on the results of this work, we anticipate the sputtered films providing comparable or even better results than we can obtain with the ALD films. Additional steps will be required to test the integration of the sputtered platinum films, as other factors such as film adhesion become important during integration.